Optical microdisk resonator with a small scatterer

C.P. Dettmann[1,3], G. V. Morozov[1], M. Sieber[1] and H. Waalkens[1,2]

[1]Department of Mathematics, University of Bristol, UK; [2]Department of Mathematics, University of Groningen, NL
[3]Presenting author, http://www.maths.bris.ac.uk/∼macpd/

1. Introduction

An optical *microresonator* is a device of micron size that partially traps light. A *microlaser* is a laser (pumped active medium that emits coherent light) designed using a microresonator. Lasers have a multitude of uses from reading DVDs to welding. The design of very efficient, very small and very directional laser emission is of major industrial interest. Aiming for lasers with these characteristics, we look for resonances (decaying, unstimulated, linear modes) with high Q-factor and Directivity (definitions below).

The most common resonator geometry is Fabry-Perot, consisting of two parallel mirrors. More recently, resonators have been designed using total internal reflection [1], which allows higher reflectivity in a smaller device, and does not fix the wavelength unlike parallel mirrors based on Bragg reflection. Many geometries are possible, for example a thin circular disk embedded in a material of lower refractive index.

The classical (ray-optics) picture is helpful here: a classical orbit is a trajectory in a 2D or 3D billiard, with the condition that it will escape if it hits the boundary at too large an angle. The circular billiard has many orbits that never escape, called *whispering gallery* orbits; it has a high Q-factor, however due to symmetry its directivity is very low. Perturbing the shape of the boundary improves the directivity, but at the expense of the Q-value.

We can keep both high Q-factor and directivity by putting an obstacle in the interior of the disk. This could be a point, line or hole [2,3], but we prefer a point (physically very small defect or hole) for which a lot more can be done analytically, and which suffices to give good directivity (below).

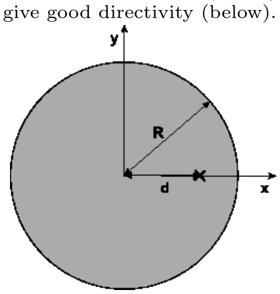

Fig 1: Microdisk parameters

2. Unperturbed microdisk

For a thin passive microdisk, Maxwell's equations reduce approximately to the 2D scalar Helmholtz equation in the plane of the microdisk

$$(\nabla^2 + k^2 n_{\text{eff}}(\mathbf{r})^2)\Psi = 0 \tag{1}$$

Here n_{eff} is the effective refractive index (a function of the true refractive index and thickness) which we take to be n inside the disk and 1 outside. $k = \omega/c$ is the wavenumber, which for resonances is analytically continued into the lower complex half-plane. Ψ is the field variable, equal to E_z for TM modes ($H_z = 0$) or H_z/n_{eff} for TE modes ($E_z = 0$). Other components of the field may be obtained by differentiating Ψ.

The unperturbed circle is separable in polar coordinates (r, φ) leading to modes with $e^{\pm im\varphi}$ dependence multiplied by $J_m(knr)$ inside the microdisk and $H_m(kr)$ outside. J and H are Bessel and Hankel functions of the first kind, respectively, to satisfy boundary conditions at the origin and at infinity. $m = 0, 1, 2, \ldots$, with $m > 0$ modes being twofold degenerate. We use the radial modal index $q = 1, 2, 3, \ldots$ to label different resonances with the same m.

The Green function for the microdisk $G(\mathbf{r}, \mathbf{r}_0, k)$ is given by (see Ref. [4])

$$\begin{aligned} -\frac{i}{4}H_0(kn|\mathbf{r}-\mathbf{r}_0|) + \frac{i}{4}\sum\nolimits_{m=0}^{\infty}\frac{D_m}{A_m}\epsilon_m \\ \times \cos[m(\varphi-\varphi_0)]\, J_m(knr_<)\, J_m(knr_>) \end{aligned} \tag{2}$$

for r and r_0 both less than R,

$$\begin{aligned} \frac{1}{2\pi kR}\sum\nolimits_{m=0}^{\infty}\frac{1}{A_m}\epsilon_m \\ \times \cos[m(\varphi-\varphi_0)]\, J_m(knr_<)\, H_m(kr_>) \end{aligned} \tag{3}$$

for one of r and r_0 greater than R,

$$\begin{aligned} -\frac{i}{4}H_0(kn|\mathbf{r}-\mathbf{r}_0|) + \frac{i}{4}\sum\nolimits_{m=0}^{\infty}\frac{B_m}{A_m}\epsilon_m \\ \times \cos[m(\varphi-\varphi_0)]\, H_m(kr_<)\, H_m(kr_>) \end{aligned} \tag{4}$$

for r and r_0 both greater than R, where $r_<$ ($r_>$) is the smaller (larger) of r and r_0. The coefficients are $\epsilon_m = 2 - \delta_{m,0}$ and

$$\begin{aligned} A_m &= \alpha_1 J_m(knR)\, H_m'(kR) - \alpha_2 J_m'(knR)\, H_m(kR) \\ B_m &= \alpha_1 J_m(knR)\, J_m'(kR) - \alpha_2 J_m'(knR)\, J_m(kR) \\ D_m &= \alpha_1 H_m(knR)\, H_m'(kR) - \alpha_2 H_m'(knR)\, H_m(kR) \end{aligned}$$

with (α_1, α_2) given by $(1, n)$ for TM and $(n, 1)$ for TE. The resonances are given by the poles of the Green function, ie $A_m = 0$ which is the matching condition between the two regions.

In the semiclassical limit $kR \gg m$ we find resonances at

$$kR \approx \frac{\pi}{n}\left(\frac{m}{2} - \frac{3}{4} - q\right) + \frac{i}{2n}\ln\left(\frac{n-1}{n+1}\right) \tag{5}$$

If instead we take $n \to \infty$ we find that kR approaches the real axis at zeros of J_{m-1} for the TM case and J_m for the TE case.

3. Perturbed microdisk

We have previously considered the case of a point scatterer using self-adjoint extension theory [4]. The equation for the resonance is $G_r(\mathbf{d}, \mathbf{d}, k_{\text{res}}) = \lambda^{-1}$ where G_r is a regularised Green function evaluated at the location of the scatterer $\mathbf{d}$, and λ is a parameter related to the strength of the scatterer. The results were similar to those below.

Here we use an explicit small scatterer of radius a and effective refractive index n_a at a point $\mathbf{d}$ inside the microdisk. For brevity we restrict to the TM case. The Green function of the perturbed disk is found by treating the scatterer in the s-wave approximation. This results in

$$\begin{aligned} G^a(\mathbf{r}, \mathbf{r}_0, k) &\approx G(\mathbf{r}, \mathbf{r}_0, k) \\ &+ \frac{G(\mathbf{r}, \mathbf{d}, k)\mathcal{D}G(\mathbf{d}, \mathbf{r}_0, k)}{1 - \mathcal{D}G^{\text{sc}}(\mathbf{d}, \mathbf{d}, k)}, \end{aligned} \tag{6}$$

where G^{sc} is the Green function in (2) without the H_0 Hankel function. The diffraction coefficient has the form $\mathcal{D} = -4i\mathcal{B}_0/\mathcal{A}_0$, where $\mathcal{A}_m$ and $\mathcal{B}_m$ are given by A_m and B_m with $(\alpha_1, \alpha_2) = (n, n_a)$, and R replaced by a. The resonances of the perturbed system are determined by the poles of the Green function and hence are defined by the equation

$$0 = -\frac{\mathcal{A}_0}{\mathcal{B}_0} + \sum\nolimits_{m=0}^{\infty}\frac{C_m}{A_m}\epsilon_m J_m^2(knd)\,. \tag{7}$$

The corresponding field Ψ follows from the residua of (6) as $\Psi(\mathbf{r}) = NG(\mathbf{r}, \mathbf{d}, k)$ where N is a normalization factor and k is the wavenumber of the resonance. Outside of the microdisk, i.e. in the region $r > R$, the field is then of the form

$$\begin{aligned} \Psi = &\frac{N}{2\pi kR}\sum\nolimits_{m=0}^{\infty}\frac{\epsilon_m \cos(m\varphi)\, J_m(knd)}{A_m} \\ &\times H_m(kr)\,, \end{aligned} \tag{8}$$

if the scatterer is located on the positive x-axis. The s-wave approximation is valid if $|nk(R-d)| \gg 1$ and $\mathcal{A}_0/\mathcal{B}_0 \ll \mathcal{A}_1/\mathcal{B}_1$.

4. Results

As noted above, we are interested in high $Q = |\Re(k)/2\Im(k)|$ and high directivity

$$D = \frac{2\pi|f(\varphi_{\max})|^2}{\int_0^{2\pi}|f(\varphi)|^2 d\varphi} \tag{9}$$

where the field at infinity takes the form $\Psi \sim f(\varphi)e^{ikr}/\sqrt{r}$.

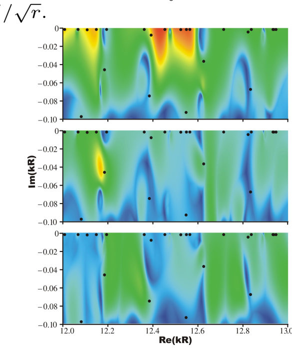

Fig 2: Directivity (red=high) and resonances for $R = 1$, $n = 3$, $a = 0.01$, $n_a = 1$. d is 0.5 (top), 0.7 (middle) and 0.9 (bottom).

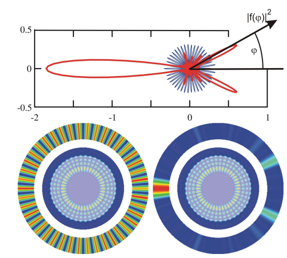

Fig 3: Field distribution of unperturbed mode $kR = 12.54876 - 10^{-6}i$ (blue at top and bottom left) and perturbed mode $kR = 12.54905 - 1.3 \times 10^{-5}i$ (red at top and bottom right). Parameters are as for the top of Fig 2; if distances are in microns, this value of k is in the visible part of the spectrum.

The directivity is remarkable given the small size of the scatterer. Two observations can help to understand this:

1. The location of the scatterer at $d = 0.5$ is the point at which a parallel beam of light at infinity would focus according to ray optics in the paraxial approximation. Compare the different sections of Fig. 2.

2. The size of the scatterer appears only logarithmically in the expressions.

This gives a definite prediction of where to put the scatterer in the case $n > 2$, which would be good to test experimentally. There is much left for future exploration, including further analytics, other geometries, and extending the s-wave and effective refractive index approximations.

Acknowledgements

This work was funded by the EPSRC, grant EP/C515137/1

References

[1] T. M. Benson, S. B. Boriskina, P. Sewell, A. Vukovic, S. C. Greedy, and A. I. Nosich. *Fron- tiers in Planar Lightwave Circuit Technology, volume 216 of NATO Science Series II: Mathematics, Physics and Chemistry*, section Micro-optical resonators for microlasers and integrated optoelectronics, pages 39-70. Springer, 2006.

[2] V. M. Apalkov and M. E. Raikh. Phys. Rev. B, **70**, 195317 (2004).

[3] J. Wiersig and M. Hentschel. Phys. Rev. A, **73** 031802(R) (2006).

[4] C. P. Dettmann, G. V. Morozov, M. M. A. Sieber, and H. Waalkens Europhys. Lett. **82**, 34002 (2008).